Bioorganic & Medicinal Chemistry Letters xxx (2018) xxx–xxx

Contents lists available at ScienceDirect

Bioorganic & Medicinal Chemistry Letters

journal homepage: www.elsevier.com/locate/bmcl

Discovery of novel 2-substituted-4-phenoxypyridine derivatives as potential antitumor agents

Yongli Duan [a,c], Shan Xu [a,c], Hehua Xiong [a], Linxiao Wang [a], Bingbing Zhao [a], Ping Wang [a], Caolin Wang [a], Yiqing Peng [a], Shifan Cai [a], Rong Luo [b], Pengwu Zheng [a,*], Qidong Tang [a,*]

[a] Jiangxi Provincial Key Laboratory of Drug Design and Evaluation, School of Pharmacy, Jiangxi Science & Technology Normal University, Nanchang 330013, PR China
[b] Jiangxi Province Institute of Materia Medica, Nanchang 330000, PR China

ARTICLE INFO

Article history:
Received 14 October 2017
Revised 25 December 2017
Accepted 28 December 2017
Available online xxxx

Keywords:
Synthesis
4-Phenoxypyridine derivatives
1,8-Naphthyridinone
Antiproliferative activity
c-Met
Flt-3

ABSTRACT

A series of 2-substituted-4-phenoxypyridine derivatives were designed, synthesized, and evaluated for their antiproliferative activity against 4 cancer cell lines (A549, HT-29, H460, and U87MG) *in vitro*. Most compounds showed moderate to excellent potency. Nine tyrosine kinases (c-Met, Flt-3, ALK, VEGFR-2, VEGFR-3, PDGFR-α, PDGFR-β, c-Kit, and EGFR) were used to evaluate the inhibitory activities with the most promising analogue **39**, which showed the Flt-3/c-Met IC_{50} values of 2.18/2.61 nM. Structure-activity relationship studies indicated that n-Pr served as R^1 group showed a higher preference, and stronger mono-EWGs on the phenyl ring (such as R^2 = 4-F) was benefited to the potency.

Cancer is one of the leading causes of morbidity and mortality worldwide, which is the second leading cause of death globally. Cancer was responsible for 8.8 million deaths in 2015. Globally, nearly 1 in 6 deaths is due to cancer.[1] Despite the efforts to discover and develop small molecule anticancer drugs in the last decades,[2–4] development of new antitumor agents with improved tumor efficiency, selectivity, and safety remains in urgent need.

Recently, significant progress has been made in the development of c-Met kinase inhibitors, resulting in the marketing of cabozantinib (approved on November 2012 by the U.S. FDA for the treatment of patients with progressive metastatic medullary thyroid cancer, **3**, Fig. 1) and more than 10 candidates under clinical trials.[5–7] We had analyzed the structural characteristics of these c-Met kinase inhibitors. The general structure of small-molecule c-Met kinases inhibitors was summarized as illustrated in Fig. 1, which could be divided to moiety A, B, C, and D. Judging from moiety A, many structure types of these derivatives were included, such as substituted quinoline (**1**–**3**), thieno[2,3-*b*]pyridine (**4**), pyrrolo[2,3-*b*]pyridine (**5**), and 2-amino-3-chloropyridine series (**6**).[8–14] However, the main modification of these different series of derivatives was focused on moiety C (a 5-atom linker), which has two obvious structural characteristics. One is the '5 atoms regulation', which means six chemical bonds distance existed between moiety B and moiety D; the other is the 5-atom linker containing hydrogen, oxygen, and nitrogen atoms which could form hydrogen-bond donor or acceptor.

In our previous study, we introduced 2-oxo-4-chloro-1,2-dihydroquinoline and pyridine fragments into the 5-atom linker based on the two structural characteristics, and the resulting 6,7-disubstitutedquinoline (**7**, Fig. 2) and pyrrolo[2,3-*b*]pyridine derivatives (**8**) showed excellent potency, respectively.[15,16] 1,8-Naphthyridinone fragment was widely used as a building block in the design of anticancer agents. For example, compounds **9** displayed a multitude of biological activities.[17]

In this work, 1,8-naphthyridinone was introduced to the 5-atom linker as illustrated in Fig. 3, because the carbonyl oxygen or two nitrogen atoms in 1,8-naphthyridinone as the hydrogen-bond acceptor have high ability to form hydrogen-bonding interactions with c-Met. 2-substitutedpyridine was used as moiety A. Substituted phenyl ring was reserved as moiety B and moiety D. Small substituents R^1 and R^2 were introduced to investigate their effects on activity of the target compounds. Accordingly, we designed a novel series of 2-substituted-4-phenoxypyridine derivatives bearing the 1,8-naphthyridinone fragment.

* Corresponding authors.
E-mail addresses: zhengpw@126.com (P. Zheng), tangqidongcn@126.com (Q. Tang).
[c] These authors contribute equally to this work.

https://doi.org/10.1016/j.bmcl.2017.12.063
0960-894X/

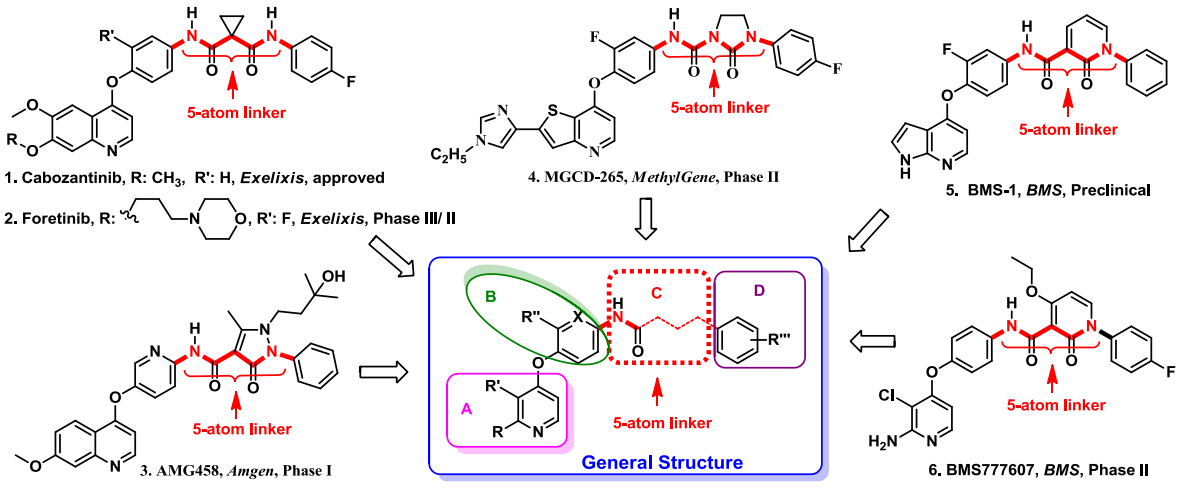

Fig. 1. The representative small-molecule c-Met kinase inhibitors and the summarized General Structure.

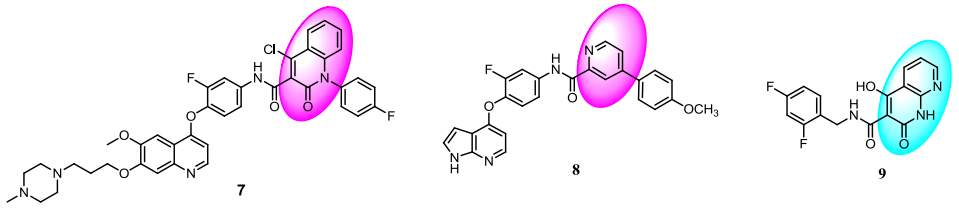

Fig. 2. Antiproliferative agents bearing 2-oxo-4-chloro-1,2-dihydroquinoline (**7**) and pyridine (**8**) in our previous work; potent drug bearing 1,8-naphthyridinone fragment (**9**).

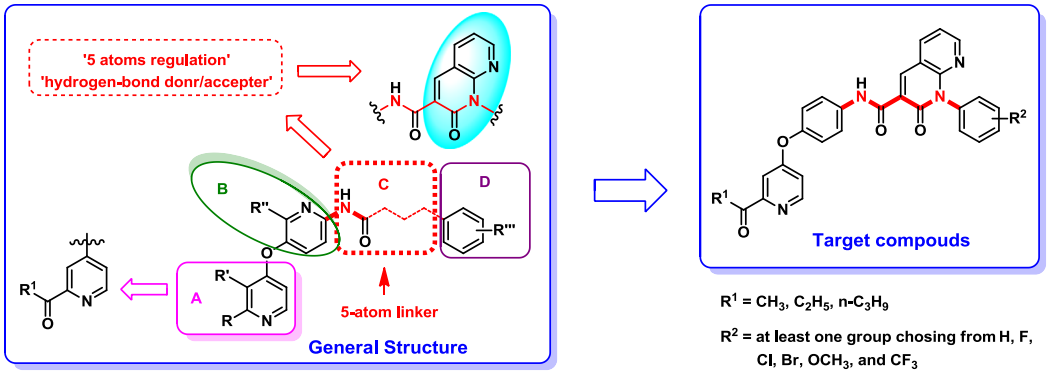

Fig. 3. Design strategy for the 2-substituted-4-phenoxypyridine derivatives bearing 1,8-naphthyridinone fragment.

The antiproliferative effect of the target compounds **19**–**45** were evaluated on the growth of four cell lines *in vitro*,[18,19] namely human lung adenocarcinoma (A549), human colon cancer (HT-29), human lung cancer (H460), and human glioblastoma (U87MG). A549, HT-29, MKN-45, and U87MG are all high expressing cell lines of c-Met kinase.[18,20] There is no overexpression of c-Met in H460 cell line, we chose it to investigate whether these compounds showed potent antiproliferative against the cell line. Moderate to excellent growth inhibition was observed for most of the compounds, and 11 of these compounds were more potent than foretinib against one or more cell lines. Furthermore, seven compounds were chosen for further evaluation of c-Met kinase inhibitory activity *in vitro*. To examine the selectivity, compound **39** was chosen to screen against 8 other tyrosine kinases. To further elucidate the binding mode of these 2-substituted-4-phenoxypyridine derivatives, docking analysis was performed using compound **39**.

The key intermediates 4-(4-amino-2-substitutedphenoxy)-*N*-substituted picolinamide **12a**–**c** were prepared as illustrated in Scheme 1. Catalyzed by NaBr, chlorination of the commercially available 2-picolinic acid with thionyl chloride resulted in the intermediate **10**. Acylation of acyl chloride **10** with amines (methylamine, ethylamine, and propanamine) in the presence of Et_3N proceeded smoothly to yield **11a**–**c**. Etherification of 4-aminophenol with **11a**–**c** catalyzed by potassium *t*-butoxide to give the key intermediates **12a**–**c**.

The target compounds **19**–**45** were prepared as illustrated in Scheme 2. Condensation of substituted aniline with 2-chloronicotinic acid in AcOH at 100 °C resulted in high yield of intermediates **13a**–**i** as white solids. **13a**–**i** were reduced by $LiAlH_4$ in THF to

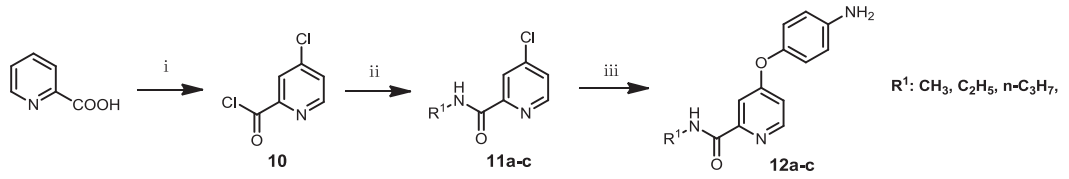

Scheme 1. Reagents and conditions: (i) $SOCl_2$, NaBr, PhCl, 55 °C, 1 h, reflux, 18 h; (ii) amines, Et_3N, THF, 0 °C, 3 h; (iii) 4-aminophenol, potassium *t*-butoxide, KI, 80 °C, 4.5 h.

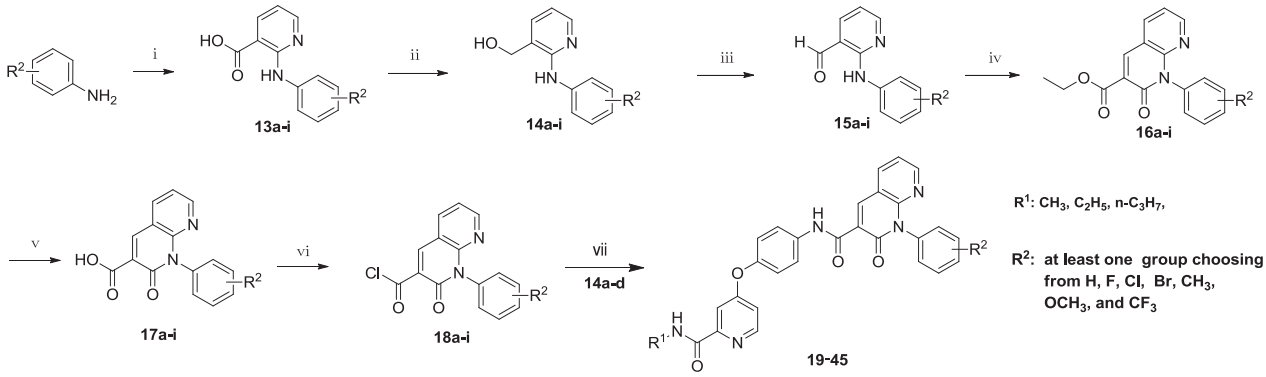

Scheme 2. Reagents and conditions: (i) 2-chloronicotinic acid, AcOH, 100 °C, 3–6 h; (ii) $LiAlH_4$, N_2, THF, r.t. 3.5 h; (iii) Pyridinium dichromate, CH_2Cl_2, r.t. 5–7 h; (iv) Dimethyl malonate, piperidine, EtOH, reflux, 30–35 h; (v) K_2CO_3, 1,4-dioxane/H_2O, 80 °C, 4–5 h (vi) $SOCl_2$, reflux, 6 h; (vii) Appropriate aniline, carbonyl chloride, DIPEA, CH_2Cl_2, 0 °C, 1 h, r.t., 5–8 h.

afford intermediates **14a–i** as white solids, which were oxidized by pyridinium dichromate to get intermediates **15a–i**. Acylation of the **15a–i** with dimethyl malonate in the presence of piperidine in refluxing EtOH yielded ethyl 2-oxo-1-substitutedphenyl-1,2-dihydro-1,8-naphthyridine-3-carboxylates **16a–i**. Simple procedures such as hydrolysis and acyl chlorination were used to convert ethyl **16a–i** to the corresponding acyl chloride **18a–i**, proceeded with K_2CO_3 and thionyl chloride, respectively. Reaction of anilines **12a–c** with acyl chloride **18a–i** promoted by DIPEA in dichloromethane at room temperature yielded the target compounds **19–45**.[21,22]

The antiproliferative activity of these novel 2-substituted-4-phenoxypyridine derivatives bearing 1,8-naphthyridinone moiety have been evaluated against the H460 and HT-29 cell lines using the MTT assay.[23] Some potent compounds were further evaluated against the A549 and U87MG cell lines. The results expressed as IC_{50} values are shown in Table 1 as the mean values of triplicate experiments.

As illustrated in Table 1, all target compounds **19–45** were found to be active against different cancer cells with potencies in the single-digit μM range. 11 of these compounds were more potent than foretinib against one or more cell lines. The IC_{50} values of the most promising compound **39**[24] were 0.062, 0.084, 0.12, and 0.96 μM against the A549, HT29, H460, and U87MG cell lines, respectively. The data indicated that it's a good design strategy to use 2-substitutedpyridine as moiety A and introduce 1,8-naphthyridinone fragment to moiety C to form the 5-atom linker.

According to the data shown in Table 1, the cell lines data revealed a preference for activity when the R^1 group was n-Pr instead of Me or Et, indicating that introduction of proper flexible terminal chain on moiety A had a positive effect. For example, the IC_{50} value of compound **37**, 0.095 μM, was lower than that of **19** and **28** against A549 cells, 0.20 μM and 0.16 μM, respectively.

Further analysis clearly revealed that different antiproliferative activities were observed when various R^2 groups were introduced into the phenyl ring (moiety D). Compound **19**, with no substituent on the phenyl ring, displayed strong antiproliferative activity with an IC_{50} of 0.20 μM against A549 cells. The introduction of stronger mono-electron-withdrawing groups (mono-EWGs) at 4-position of the phenyl ring (**21**, R^2 = 4-F, IC_{50} = 0.11 μM) led to an improvement on antiproliferative activity, which could be further confirmed by compounds **30** and **39**. However, the introduction of mono-EWGs (**20**, R^2 = 2-F, IC_{50} = 0.61 μM) or mono-electron-donating groups (mono-EDGs, **24**, R^2 = 4-OCH_3, IC_{50} = 3.11 μM) at other position reduced the activities. Moreover, double electron-withdrawing groups (double-EWGs) could decrease the potency of the compounds. For example, the inhibitory efficacy of **34** (R^2 = 2-F-4-Br, IC_{50} = 1.82 μM) and **35** (R^2 = 2-Cl-4-CF_3, IC_{50} = 3.29 μM) are 11.4 times and 20.1 times lower than **28** (R^2 = H, IC_{50} = 0.16 μM), respectively.

The c-Met enzymatic assays of seven 2-substituted-4-phenoxypyridine derivatives were evaluated using homogeneous time-resolved fluorescence (HTRF) assay.[25] The results suggested that the inhibition of c-Met may be one mechanism of the antiproliferative effect of these derivatives (Table 2). Compound **39** showed the most potent activity with an IC_{50} value of 2.61 nM, which was comparable to that of the positive control foretinib (IC_{50} = 1.93 nM), and this compound should be studied further.

As shown in Table 3, compound **39** was chosen for further evaluation of the selectivity on c-Met over other tyrosine kinases. Compared with its high potency against c-Met (IC_{50} = 2.61 nM), **39** also exhibited high inhibitory effects against Flt-3 (IC_{50} = 2.18 nM) and VEGFR-3 (IC_{50} = 23.6 nM). While, **39** showed weak potency on ALK, VEGFR-2, PDGFR-β, c-Kit, PDGFR-α, and EGFR. These data suggested that compound **39** is a promising multitarget kinase inhibitor.

To further elucidate the binding mode of the target compounds, three-dimensional structure of the c-Met (PDB code: 3LQ8) and Flt-3 (PDB code: 4XUF) was obtained from RCSB Protein Data Bank. Docking simulation was conducted using SURFLEX-DOCK module

Table 1
Antiproliferative activities of the target compounds **19**–**45** against the A549, HT-29, H460, and U87MG cancer cell lines *in vitro*.

Compd.	R^1	R^2	IC_{50} (μM)			
			A549	HT-29	H460	U87MG
19	Me	H	**0.20 ± 0.053** [a]	**0.25 ± 0.036**	**0.32 ± 0.049**	1.82 ± 0.27
20	Me	2-F	0.61 ± 0.050	**0.26 ± 0.016**	0.59 ± 0.012	3.36 ± 0.30
21	Me	4-F	**0.11 ± 0.026**	**0.16 ± 0.018**	**0.21 ± 0.032**	2.91 ± 0.52
22	Me	4-Cl	0.37 ± 0.016	0.39 ± 0.012	ND [b]	ND
23	Me	4-Br	1.05 ± 0.10	1.18 ± 0.28	3.71 ± 0.30	15.03 ± 1.31
24	Me	4-OCH_3	3.11 ± 0.12	0.92 ± 0.013	ND	ND
25	Me	2-F-4-Br	1.42 ± 0.15	1.95 ± 0.22	ND	ND
26	Me	2-Cl-4-CF_3	2.09 ± 0.21	3.19 ± 0.45	2.11 ± 0.19	19.82 ± 1.63
27	Me	3-Cl-4-F	1.56 ± 0.17	1.81 ± 0.24	ND	ND
28	Et	H	**0.16 ± 0.040**	**0.22 ± 0.027**	1.12 ± 0.21	2.65 ± 0.30
29	Et	2-F	0.49 ± 0.061	**0.26 ± 0.032**	1.23 ± 0.15	3.25 ± 0.63
30	Et	4-F	**0.12 ± 0.047**	**0.19 ± 0.042**	**0.22 ± 0.025**	**1.13 ± 0.11**
31	Et	4-Cl	**0.25 ± 0.039**	0.33 ± 0.024	ND	ND
32	Et	4-Br	0.91 ± 0.032	1.16 ± 0.40	ND	ND
33	Et	4-OCH_3	2.01 ± 0.29	3.35 ± 0.16	1.72 ± 0.33	7.21 ± 0.39
34	Et	2-F-4-Br	1.82 ± 0.18	2.07 ± 0.23	1.79 ± 0.19	10.26 ± 1.01
35	Et	2-Cl-4-CF_3	3.29 ± 0.41	4.77 ± 0.56	ND	ND
36	Et	3-Cl-4-F	1.92 ± 0.22	2.60 ± 0.21	ND	ND
37	n-Pr	H	**0.095 ± 0.0035**	**0.098 ± 0.0061**	**0.11 ± 0.039**	1.51 ± 0.12
38	n-Pr	2-F	**0.15 ± 0.065**	**0.20 ± 0.082**	0.39 ± 0.043	2.32 ± 0.19
39	n-Pr	4-F	**0.062 ± 0.0051**	**0.084 ± 0.0069**	**0.12 ± 0.021**	**0.96 ± 0.036**
40	n-Pr	4-Cl	**0.12 ± 0.052**	0.39 ± 0.038	ND	ND
41	n-Pr	4-Br	0.15 ± 0.041	0.53 ± 0.084	0.62 ± 0.036	5.19 ± 0.54
42	n-Pr	4-OCH_3	0.82 ± 0.050	1.56 ± 0.64	1.73 ± 0.58	8.21 ± 0.61
43	n-Pr	2-F-4-Br	1.31 ± 0.26	2.16 ± 0.37	ND	ND
44	n-Pr	2-Cl-4-CF_3	1.25 ± 0.28	1.96 ± 0.14	3.17 ± 0.64	10.92 ± 1.06
45	n-Pr	3-Cl-4-F	0.59 ± 0.025	0.92 ± 0.070	1.60 ± 0.51	3.59 ± 0.34
Foretinib [c]			0.26 ± 0.029	0.29 ± 0.018	0.36 ± 0.021	1.35 ± 0.10

[a] Bold values show the IC_{50} values of the target compounds lower than the values of the positive control.
[b] ND: Not determined.
[c] Used as the positive control.

of SYBYL 8.1 package version. The shape and properties of the receptor are represented on a grid by several different sets of fields that provide more accurate scoring of the ligand poses. The binding model was exemplified by the interaction of compound **39** with c-Met (Fig. 4A) and Flt-3 (Fig. 4B). As shown in Fig. 4A, the nitrogen atom of pyridine ring and the adjacent oxygen atom of amide bond in compound **39** formed two hydrogen-bonding interactions with MET1160. In the 5-atom linker, hydrogen/oxygen atom of amide bond and oxygen atom of 1,8-naphthyridin-2-one formed three hydrogen bonds with ASP1222 and LYS1110. As we can see, five H-bonds were formed. In the c-Met enzymatic assays, compound **39** showed the most potent activity with an IC_{50} value of 2.61 nM, which is consistent with the docked model depicted in Fig. 4A. In Fig. 4B, oxygen atom of amide bond connected with pyridine ring of compound **39** formed hydrogen-bonding interactions with CYS694. In the 5-atom linker, hydrogen and oxygen atom of amide bond formed two hydrogen bonds with GLU661 and ASP829, respectively. Three hydrogen-bonding interactions were formed, which is consistent with the IC_{50} value of 2.18 nM against Flt-3. Therefore, Compound 39 was bound well with c-Met and Flt-3.

Table 2
c-Met kinase activity of selected compounds **19**, **21**, **28**, **30**, **37**, **38**, **39** and foretinib *in vitro*.

Compd.	IC_{50} on c-Met (nM)
19	7.06
21	16.29
28	12.53
30	8.24
37	9.89
38	8.32
39	2.61
Foretinib	1.93

Table 3
Inhibition of tyrosine kinases by compound **39**.

Kinase	Enzyme IC_{50} (nM)
Flt-3	2.18
VEGFR-3	23.6
ALK	186.2
VEGFR-2	291.3
PDGFR-β	482.1
c-Kit	529.3
PDGFR-α	691.5
EGFR	>100,000

In summary, a total of 27 novel 2-substituted-4-phenoxypyridine derivatives bearing 1,8-naphthyridinone fragment were designed and synthesized. 4 human cancer cell lines were used to evaluate the antiproliferative potency of the synthesized compounds. 11 of these compounds were more potent than foretinib against one or more cell lines. Compound **39** (Flt-3/c-Met IC_{50} = 2.18/2.61 nM, a multi-target tyrosine kinase inhibitor) showed the strongest antiproliferative activities against A549, HT29, H460, and U87MG cell lines (IC_{50} values: 0.062, 0.084, 0.12, and 0.96 μM, respectively). Analysis of SARs indicated that n-Pr served as R^1 group showed a higher preference, and stronger mono-EWGs at 4-position (such as R^2 = 4-F) of the phenyl ring (moiety D) was benefit to improve the inhibitory activity of the target compounds.

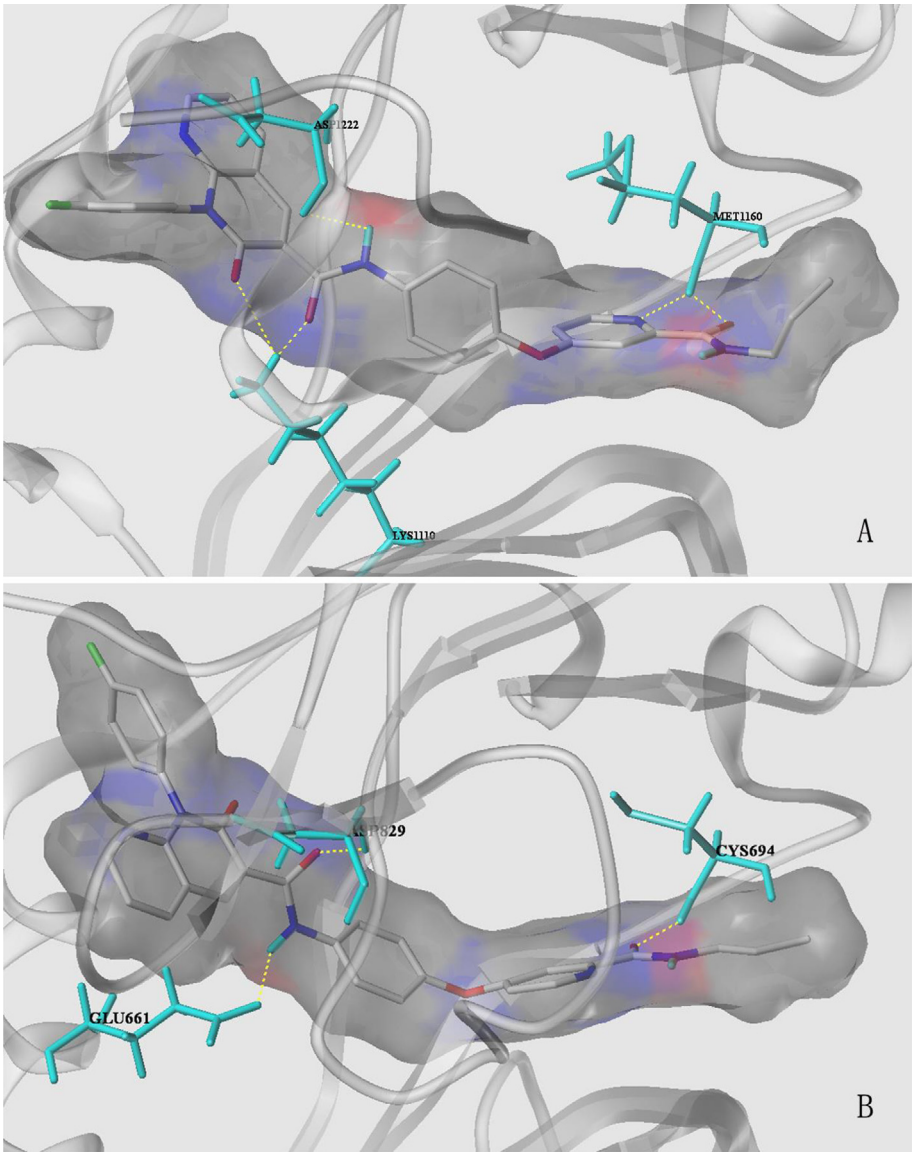

Fig. 4. Binding poses of compound **39** with c-Met (A) and Flt-3 (B). The proteins were displayed by grid ribbon. Compound **39** was displayed by multicolor sticks. H-bonding interactions between compound **39** and c-Met/Flt-3 were indicated with dashed yellow lines.

Acknowledgments

We gratefully acknowledge the generous support provided by National Natural Science Foundation of China (NSFC No. 81660572), Natural Science Foundation of Jiangxi Province (20171BAB215071), Top-notch talent project of Jiangxi Science & Technology Normal University (2016QNBJRC002), and Jiangxi Provincial Key Laboratory of Drug Design and Evaluation (20171BCD40015).

A. Supplementary data

Supplementary data associated with this article can be found, in the online version, at https://doi.org/10.1016/j.bmcl.2017.12.063.

References

1. http://www.who.int/mediacentre/factsheets/fs297/en/ [WHO Media Centre, Cancer, Updated February, 2017, last accessed: 10/12/2017].
2. Hoelder S, Clarke PA, Workman P. *Mol Oncol*. 2012;6:155.
3. Dayyani F, Gallick GE, Christopher CL, Corn PG. *J Natl Cancer Inst*. 2011;103:1665.
4. You WK, Sennino B, Williamson CW, et al. *Cancer Res*. 2011;71:4758.
5. Kataoka Y, Mukohara T, Tomioka H, et al. *Invest New Drugs*. 2012;30:1352.
6. Zillhardt M, Park SM, Romero IL, et al. *Clin Cancer Res*. 2011;17:4042.
7. Cecchi F, Rabe DC, Bottaro DP. *Eur J Cancer*. 2010;46:1260.
8. Norman MH, Liu LB, Lee M, et al. *J Med Chem*. 2012;55:1858.
9. Schroeder GM, An Y, Cai ZW, et al. *J Med Chem*. 2009;52:1251.
10. Kim KS, Zhang L, Schmidt R, et al. *J Med Chem*. 2008;51:5330.
11. Yakes FM, Chen J, Tan J, et al. *Mol Cancer Ther*. 2011;10:2298.
12. D'Angelo ND, Bellon SF, Booker SK, et al. *J Med Chem*. 2008;51:5766.
13. Liu XD, Newton RC, Scherle PA. *Trends Mol Med*. 2009;16:1471.
14. Kung PP, Funk L, Meng J, Alton G, Padrique E, Mroczkowski B. *Eur J Med Chem*. 2008;43:1321.
15. Tang QD, Zhai X, Tu YY, et al. *Bioorg Med Chem Lett*. 2016;26:1794.
16. Zhu WF, Wang WH, Tang QD, et al. *Bioorg Med Chem*. 2016;24:812.
17. Zhao XZ, Smith SJ, Métifiot M, et al. *J Med Chem*. 2014;57:1573.
18. Takayuki N, Osamu T, Atsumi Y, et al. *Cancer Sci*. 2010;101:210.
19. Tiedt R, Degenkolbe E, Furet P, et al. *Cancer Res*. 2011;71:5255.
20. Ted LU, Torsten H, Sheila JM. *Anticancer Agent Med*. 2010;10:7.
21. Tang QD, Zhao YF, Du XM, Chong LE, Gong P, Guo C. *Eur J Med Chem*. 2013;69:77.
22. Tang QD, Duan YL, Wang LX, et al. *Eur J Med Chem*. 2018;143:266.
23. *Cytotoxicity assay*: A standard MTT assay was used to measure cell growth. Cancer cell lines were cultured in minimum essential medium (MEM) supplemented with 10% fetal bovine serum (FBS). Approximate 4×10^3 cells,

suspended in MEM medium, were plated onto each well of a 96-well plate and incubated in 5% CO_2 at 37 °C for 24 h. The compounds tested at the indicated final concentrations were added to the culture medium and the cell cultures were continued for 72 h. Fresh MTT was added to each well at a terminal concentration of 5 μg/mL, and incubated with cells at 37 °C for 4 h. The formazan crystals were dissolved in 100 mL DMSO of each well, and the absorbency at 492 nm (for absorbance of MTT formazan) and 630 nm (for the reference wavelength) was measured with an ELISA reader. All of the compounds were tested in triplicate in each cell line. The results expressed as IC_{50} were the average of three determinations and calculated by using the Bacus Laboratories Incorporated Slide Scanner software.

24. *The procedure for preparation of compound **39**:* To the mixture of picolinic acid (5.00 g, 0.04 mol), sodium bromide (0.42 g, 0.004 mol), and chlorobenzene (40 mL), dilute thionyl chloride was added slowly with stirring maintaining the temperature at 55 °C. The temperature was raise to 85 °C to stir for 18 h. Reaction was complete by TLC analysis. Filtration was used to remove solids. The filtrate was concentrated under reduced pressure to afford 4-chloropicolinoyl chloride as a yellow viscous oil, which was used for next step without further purification. 4-chloropicolinic acid chloride (3.00 g, 0.017 mol) and n-propylamine were added sequentially to tetrahydrofuran (30 mL). The reaction was stirred at 0 °C for 3 h. The reaction was completed by TLC analysis. The reaction mixture was added to a suitable amount of water and extracted 2–3 times with ethyl acetate. The organic phase was concentrated under reduced pressure to give 4-chloro-*N*-propylpicolinamide as a yellow viscous oil. 4-Aminophenol (2.50 g, 0.023 mol) and potassium tert-butoxide (3.39 g, 0.03 mol) were added to dimethyl sulfoxide (DMSO), and stirred at room temperature under a nitrogen atmosphere for 1 h. 4-Chloro-*N*-propylpicolinamide (3.00 g, 0.015 mol) and potassium iodide (0.33 g, 0.002 mol) was dissolved in DMSO (30 mL) and stirred at room temperature for 30 min, which was added drop wise to the former mixture and stirred at 80 °C for 4.5 h. The reaction was completed by TLC analysis. The reaction solution was added to sodium chloride and extracted with ethyl acetate. The organic layer was dried over anhydrous sodium sulfate and concentrated under reduced pressure to give 4-(4-aminophenoxy)-*N*-propylpicolinamide as a yellow viscous oil. 2-oxo-1-(4-fluorophenyl)-1,2-dihydro-1,8-naphthyridine-3-carbonyl chloride were synthesized according our previously reported procedures in Ref. 20. The crude product was purified by chromatography on silica gel using $MeOH/CH_2Cl_2$ to afford the target compounds **39** as white solids. Yield: 59%. ^1H NMR (400 MHz, DMSO-d_6) δ 11.80 (s, 1H), 9.17 (s, 1H), 8.79 (s, 1H), 8.60 (d, J = 6.0 Hz, 2H), 8.52 (d, J = 5.6 Hz, 1H), 7.89 (d, J = 8.7 Hz, 2H), 7.50–7.43 (m, 4H), 7.41 (d, J = 3.8 Hz, 2H), 7.25 (d, J = 8.6 Hz, 2H), 7.17 (d, J = 2.9 Hz, 1H), 3.21 (dd, J = 13.3, 6.6 Hz, 2H), 1.51 (dd, J = 14.3, 7.2 Hz, 2H), 0.84 (t, J = 7.3 Hz, 3H); ^{13}C NMR (100 MHz, DMSO-d_6) δ 166.32, 163.75, 163.60, 163.31, 161.16, 161.10, 153.17, 151.48, 150.99, 149.90, 144.37, 139.98, 136.39, 133.66, 131.80, 131.71, 123.33, 122.44 (2C), 122.15 (2C), 120.42, 116.78, 116.55, 115.34, 114.81, 109.62, 41.21, 22.95, 11.90; MS m/z (ESI): 538.2 $[M+H]^+$; Anal. calcd. for $C_{30}H_{24}FN_5O_4$ (%): C, 67.04; H, 4.50; N, 13.03. Found (%): C, 67.01; H, 4.47; N, 12.98.

25. *In vitro kinase assay*: The kinase assays were performed by homogeneous time-resolved fluorescence (HTRF) assay as previously reported protocol. Briefly, 20 μg/mL poly (Glu, Tyr) 4:1 (Sigma) was preloaded as a substrate in 384-well plates. Then 50 μL of 10 mM ATP (Invitrogen) solution diluted in kinase reaction buffer (50 mM HEPES, pH 7.0, 1 M DTT, 1 M $MgCl_2$, 1 M $MnCl_2$, and 0.1% NaN_3) was added to each well. Various concentrations of compounds diluted in 10 μL of 1% DMSO (v/v) were used as the negative control. The kinase reaction was initiated by the addition of purified tyrosine kinase proteins diluted in 39 μL of kinase reaction buffer solution. The incubation time for the reactions was 30 min at 25 °C, and the reactions were stopped by the addition of 5 μL of Streptavidin-XL665 and 5 μL Tk Antibody Cryptate working solution to all of wells. The plates were read using Envision (PerkinElmer) at 320 nm and 615 nm. The inhibition rate (%) was calculated using the following equation: % inhibition = 100 − [(Activity of enzyme with tested compounds − Min)/(Max − Min)] × 100 (Max: the observed enzyme activity measured in the presence of enzyme, substrates, and cofactors; Min: the observed enzyme activity in the presence of substrates, cofactors and in the absence of enzyme). IC_{50} values were calculated from the inhibition curves.